A Journal of the Gesellschaft Deutscher Chemiker
Angewandte Chemie
GDCh
International Edition
www.angewandte.org

Title: A Molecular Hybrid of an Atomically Precise Silver Nanocluster and Polyoxometalates for H2 Cleavage into Protons and Electrons

Authors: Kentaro Yonesato, Seiji Yamazoe, Daisuke Yokogawa, Kazuya Yamaguchi, and Kosuke Suzuki

To be cited as: *Angew. Chem. Int. Ed.* 10.1002/anie.202106786

Link to VoR: https://doi.org/10.1002/anie.202106786

WILEY-VCH

WILEY-VCH

COMMUNICATION

A Molecular Hybrid of an Atomically Precise Silver Nanocluster and Polyoxometalates for H_2 Cleavage into Protons and Electrons

Kentaro Yonesato,[a] Seiji Yamazoe,[b,d] Daisuke Yokogawa,[c] Kazuya Yamaguchi,*[a] and Kosuke Suzuki*[a,d]

[a] Dr. K. Yonesato, Prof. Dr. K. Yamaguchi, Dr. K. Suzuki
Department of Applied Chemistry, School of Engineering
The University of Tokyo
7-3-1 Hongo, Bunkyo-ku, Tokyo 113-8656 (Japan)
E-mail: ksuzuki@appchem.t.u-tokyo.ac.jp, kyama@appchem.t.u-tokyo.ac.jp

[b] Prof. Dr. S. Yamazoe
Department of Chemistry, Graduate School of Science
Tokyo Metropolitan University
1-1 Minami Osawa, Hachioji, Tokyo 192-0397 (Japan)

[c] Dr. D. Yokogawa
Graduate School of Arts and Science
The University of Tokyo
3-8-1 Komaba, Meguro-ku, Tokyo 153-8902 (Japan)

[d] Prof. Dr. S. Yamazoe, Dr. K. Suzuki
Precursory Research for Embryonic Science and Technology (PRESTO)
Japan Science and Technology Agency (JST)
4-1-8 Honcho, Kawaguchi, Saitama 332-0012 (Japan)

Supporting information for this article is given via a link at the end of the document.

Abstract: Atomically precise silver (Ag) nanoclusters are promising materials as catalysts, photocatalysts, and sensors because of their unique structures and mixed-valence states (Ag^+/Ag^0). However, their low stability hinders the in-depth study of their intrinsic reactivity and catalytic property accompanying their redox processes. Herein, we demonstrate that a molecular hybrid of an atomically precise $\{Ag_{27}\}^{17+}$ nanocluster and polyoxometalates (POMs) can efficiently cleave H_2 into protons and electrons. The Ag nanocluster accommodates electrons through the redox reaction from $\{Ag_{27}\}^{17+}$ to $\{Ag_{27}\}^{13+}$, and the POM ligands play the following important roles: (i) a significant stabilization of the typically unstable Ag nanocluster to preserve its structure during the redox reaction with H_2, (ii) formation of a unique interface between the Ag nanocluster and metal oxides for efficient H_2 cleavage, and (iii) storage of the generated protons on the negatively charged basic surface.

Silver (Ag) nanoclusters with well-defined molecular structures and electronic states have recently attracted great interest in diverse fields such as structural chemistry, photochemistry, catalysis, electrochemistry, and biochemistry.[1] Recently, stimulated by the first report on the crystal structure in 2011,[2a] several atomically precise Ag nanoclusters have been synthesized by employing organic protecting ligands including thiols, phosphines, and alkynes, and the correlation between their unique physicochemical properties and their structures and electronic states has been extensively explored.[2] Although the redox property and reactivity of Ag nanoclusters having mixed-valence states, *i.e.*, Ag^+/Ag^0, and atomically precise structures generate considerable interest, their low stability, which typically induces undesired decomposition and agglomeration, hinders the in-depth study of these properties involved in the redox processes.

Very recently, we reported the development of a new synthetic method for atomically precise stable Ag nanoclusters supported by lacunary polyoxometalates (POMs).[5,6] POMs are a large family of anionic metal oxide clusters that exhibit unique structures and properties including acidity/basicity and redox and photochemical properties.[3] Using lacunary POMs as inorganic multidentate ligands, various inorganic nanoclusters have been synthesized.[4] Our previously reported POM-stabilized Ag nanoclusters, which comprised an $\{Ag_{27}\}^{17+}$ nanocluster surrounded by three C-shaped $\{Si_2W_{18}O_{66}\}$ units (**Ag27**; $TBA_{16}(Me_2NH_2)_8H_5Ag_2[Ag_{27}(Si_6W_{54}O_{198})]$; TBA = $^n Bu_4N^+$; Figure 1), showed unprecedented ultrastability in both solid and solution states; the structure and electronic state of the nanocluster did not change for at least one week in organic solvents.[5] Considering that nanosized Ag catalysts on metal oxide supports exhibit catalytic activity in a variety of reactions such as oxidation, reduction, hydration, carboxylation, and alkylation,[7] the unique combination of components in atomically precise mixed-valent Ag nanoclusters stabilized by POMs could provide the hybrids with synergistic or cooperative reactivity and/or catalytic ability.

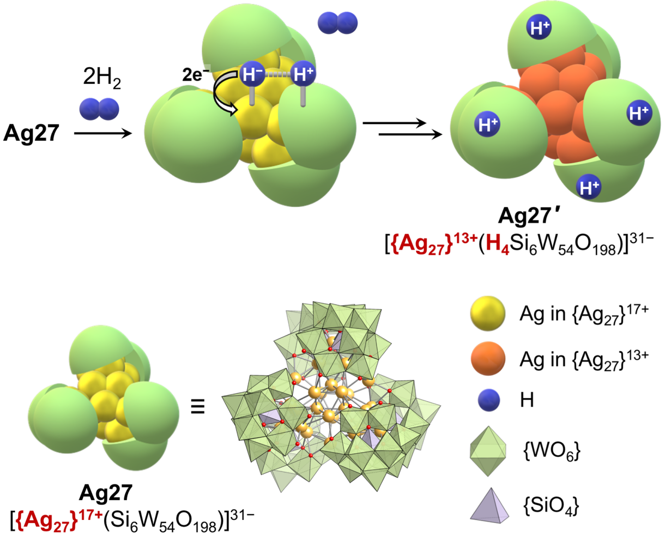

Figure 1. Schematic of the cleavage of H_2 over **Ag27** nanoclusters.

10.1002/anie.202106786

In this work, we focused on the cleavage reaction of dihydrogen (H_2) on a molecular hybrid of an Ag nanocluster and POMs. Cleavage of the H–H bond is a fundamentally important reaction that can proceed via a heterolytic or a homolytic pathway,[8–10] and it is a crucial process in the catalytic hydrogenation of organic functional groups,[7h,11–13] H_2 oxidation by hydrogenases,[14] or its model catalysts.[15] For example, metal nanoparticles on suitable metal oxide supports can efficiently cleave H_2 through a heterolytic pathway.[8,11] With regard to atomically precise nanoclusters, the unique reactivity of gold nanoclusters toward H_2[16] or hydride (H^-)[17] has been recently studied. However, although Ag nanoclusters possessing H^- ligands have been synthesized by the reaction of Ag ions and BH_4^-,[18] to the best of our knowledge, no report has dealt with the reaction of atomically precise Ag nanoclusters with H_2 or H^-, most likely due to their low stability. Herein, we report for the first time the unique reactivity of an atomically precise Ag nanocluster supported by POMs (**Ag27**) with H_2 (Figure 1). The hybrid molecular structure of $\{Ag_{27}\}^{17+}$ and POMs in **Ag27** enabled the efficient cleavage of H_2 molecules (1 atm) into protons and electrons, which were stored on the POM frameworks and the Ag nanocluster, respectively. The process involves most likely a heterolytic H_2 cleavage pathway at the interface between the Ag nanocluster and the POMs. Notably, the intrinsic structure of the Ag nanocluster was preserved even after the redox reaction of the nanocluster from $\{Ag_{27}\}^{17+}$ to $\{Ag_{27}\}^{13+}$ through the reaction with H_2. This unique reactivity of the Ag nanocluster was facilitated by the surrounding POM frameworks, which act not only as stabilizing agents for the Ag nanocluster but also as basic sites to promote the cooperative cleavage of H_2 and store the generated protons.

The UV–vis spectrum of a green solution of **Ag27** in *N,N*-dimethylformamide (DMF) showed prominent absorption bands at 420, 500 (shoulder), and 600 nm (Figures 2a and 2b). By bubbling H_2 into a solution of **Ag27** in DMF at 50°C, the color of the reaction solution changed from green to brown after 1 h (Figure 2a), and the corresponding UV–vis spectra changed significantly, exhibiting two isosbestic points at 410 and 456 nm and new absorption bands in the visible light region (400, 480, and 580 nm), whereas the absorption band at 420 nm decreased (Figure 2b). In contrast, the UV–vis spectrum of **Ag27** in DMF did not change under air at 50°C in the absence of H_2 (Figure S1). Considering that an absorption band due to surface plasmon resonance of Ag nanoparticles (~400 nm) was not observed, it can be assumed that undesirable agglomeration of $\{Ag_{27}\}$ nanoclusters into Ag nanoparticles did not occur. Additionally, the absence of an absorption band assignable to the intervalence charge transfer of W^{5+}/W^{6+} in the POMs (typically, 650–1200 nm)[19] indicates that the W^{6+} species in the POM frameworks were not reduced to W^{5+} species during the reaction with H_2. Density functional theory (DFT) calculations revealed that LUMO and LUMO+1 of **Ag27** were delocalized over $\{Ag_{27}\}$ nanocluster, which suggested the $\{Ag_{27}\}^{17+}$ could accommodate additional electrons (Figure S2).[20] The absorption bands at 420, 500 (shoulder), and 600 nm of **Ag27** can be assigned to the charge transfer from the $\{Ag_{27}\}$-based HOMO to the delocalized W5d orbitals of the POMs, the charge transfer from the $\{Ag_{27}\}$-based HOMO−1 to W5d orbitals of the POMs, and the intra-$\{Ag_{27}\}$ charge transfer from HOMO to LUMO, respectively (Figure S2). These results indicate that the changes in the UV–vis spectrum of **Ag27** after the reaction with H_2 are likely due to the change in the electronic state of the $\{Ag_{27}\}$ nanocluster.

To confirm the structure of the Ag nanocluster/POM hybrid after the reaction with H_2 (**Ag27'**), the electron spray ionization (ESI) mass spectrum of the reaction solution of **Ag27** with H_2 was measured. As described in our previous report, the ESI mass spectrum of **Ag27** showed a series of complicated sets of signals, all of which were assignable to the hybrid structure (Figure S3).[5] In contrast, after the reaction of **Ag27** with H_2, the corresponding ESI mass spectrum (negative mode) exhibited a simple prominent set of signals at around *m/z* 3592, which were assignable to the sum of two sets of signals, *i.e.*, $[\mathbf{I}+4H]^{5-}$ (calcd *m/z* 3591.892; **I** = $[TBA_6(Me_2NH_2)_2H_{16}Ag_2(Ag_{27}Si_6W_{54}O_{198})]$) and $[\mathbf{I}+4H+H_2O]^{5-}$ (calcd *m/z* 3595.494) (Figure 2c). Importantly, these results suggest that the anion structure of **Ag27** ($Ag_{27}(Si_6W_{54}O_{198})$) and two Ag^+ counter cations were preserved even after the reaction with H_2. Furthermore, to quantify the amount of H_2 molecules cleaved and hydrogen species generated, we conducted the reaction using deuterium (D_2) instead of H_2. The ESI mass spectrum of the reaction solution of **Ag27** with D_2 exhibited a similar prominent set of signals, which were shifted to higher *m/z* regions (at around *m/z* 3593) compared with those of the reaction solution using H_2 (Figure 2d, S4). This set of signals was attributable to the sum of $[\mathbf{I}+4D]$ (calcd *m/z* 3592.697) and $[\mathbf{I}+4D+D_2O]$ (calcd *m/z* 3596.701; Figure S4), thus showing that

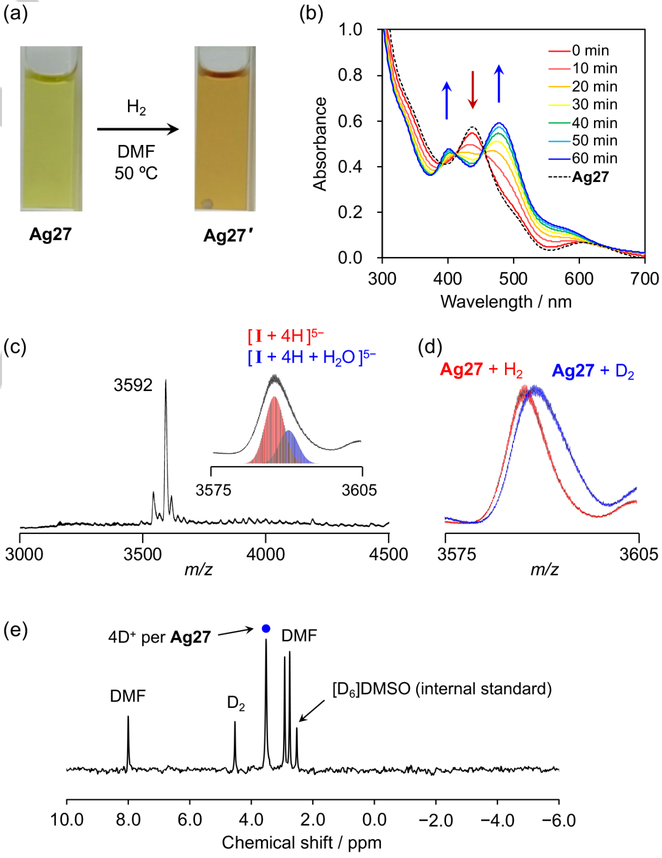

Figure 2. Change in the color (a) and the UV–vis spectra (b) of the reaction solution of **Ag27** and H_2 in DMF (10 μM, 1 cm cell) at 50°C for 1 h. (c) ESI mass spectrum (negative mode) of the reaction solution of **Ag27** and H_2 in DMF. The observed set of signals was assignable to the sum of $[\mathbf{I}+4H]^{5-}$ (**I** = $TBA_6(Me_2NH_2)_2H_{16}Ag_2(Ag_{27}Si_6W_{54}O_{198})$; calcd *m/z* 3591.892, red pattern) and $[\mathbf{I}+4H+H_2O]^{5-}$ (calcd *m/z* 3595.494, blue pattern). (d) Enlarged ESI mass spectrum (negative mode) of the solution of **Ag27** after the reaction with H_2 (red line) or D_2 (blue line) in DMF. (e) ^2H NMR spectrum of the reaction solution of **Ag27** and D_2 in DMF.

four additional H or D atoms were attached on **Ag27** by the reaction with H_2 or D_2, respectively. The ^{2}H NMR spectrum of the reaction solution of **Ag27** with D_2 showed a signal at 3.54 ppm, which was derived from D^+ produced in the cleavage reaction (Figures 2e and S5). The formation of four D^+ with respect to **Ag27** was confirmed by comparing the peak area of D atoms and that of [D_6]dimethyl sulfoxide ([D_6]DMSO, internal standard). Meanwhile, no signal attributable to deuteride (D^-) was observed. These results support the dissociation of two H_2 (or D_2) molecules into four H^+ (or D^+) and four electrons (*i.e.*, $2H_2 \rightarrow 4H^+ + 4e^-$ or $2D_2 \rightarrow 4D^+ + 4e^-$) over **Ag27**, and the generated protons (or deuterons) were probably stored on the oxygen-rich basic surface of the negatively charged POM frameworks.

Next, to elucidate where the generated electrons were stored, the electronic state and structure of **Ag27'** were investigated by Ag K-edge X-ray absorption fine structure (XAFS) studies (Figures 3a–3d). According to reported XAFS studies on metal nanoclusters,[21] all solid-state XAFS measurements were conducted at 10 K to reduce the Debye–Waller factors for a reliable analysis. The X-ray absorption near edge structure (XANES) spectrum of **Ag27'** was observed between those of **Ag27** and Ag foil, which indicates that the reduction of the $\{Ag_{27}\}$ nanocluster occurred upon the reaction with H_2 (Figure 3a). Additionally, monitoring of the reaction solution of **Ag27** with H_2 in DMF by XANES spectroscopy revealed that the absorption edge energy (E_0) changed from 25517.7 to 25517.11 eV,[22] and the absorption in the white line (~25528 eV) decreased during the reaction (Figures 3b and S6). Notably, the XANES spectrum of **Ag27'** can be fitted by linear combination of 75% of **Ag27** and 25% of Ag foil (Figure S7). Additionally, X-ray photoelectron spectroscopy (XPS) spectrum of **Ag27'** in Ag 3d region showed two peaks at 374.63 eV ($3d_{3/2}$) and 368.63 eV ($3d_{5/2}$), both of which could be fitted as a mixture of Ag^0 and Ag^+, assuming the charge of $\{Ag_{27}\}$ to be +13 (Figure S8). Based on these results and considering that the W^{6+} atoms of the POM frameworks were not reduced, it seems reasonable to conclude that the electrons generated by H_2 cleavage were stored in the $\{Ag_{27}\}$ nanocluster. Direct current magnetic susceptibility measurement revealed that **Ag27'** was diamagnetic and that its ground state was a singlet.

To gain more insight into the structure of the $\{Ag_{27}\}$ nanocluster, we conducted a solid-state Ag K-edge extended X-ray absorption fine structure (EXAFS) analysis. The *k*-space EXAFS spectrum of **Ag27'** showed oscillation patterns similar to those of **Ag27**, albeit clearly different from those of Ag foil (Figure 3c), thus indicating that the overall intrinsic structure of the $\{Ag_{27}\}$ nanocluster was preserved during the reaction. However, the oscillation patterns of **Ag27'** were slightly shifted to smaller *k* values compared with those of **Ag27**, indicating that the Ag···Ag distances within the $\{Ag_{27}\}$ nanoclusters were slightly modified by the reaction with H_2.

According to our previous single-crystal X-ray analysis of **Ag27**, the $\{Ag_{27}\}$ nanocluster was composed of three $\{Ag_6\}$ octahedrons (Ag1–Ag6, Ag7–Ag12, Ag13–Ag18), a face-sharing dioctahedral $\{Ag_9\}$ core (Ag6, Ag12, Ag18, Ag19–Ag24), and three Ag atoms (Ag25–Ag27) bridging the $\{Ag_6\}$ octahedrons (Figure 3e).[5] Although the $\{Ag_{27}\}$ nanocluster was surrounded by the rigid and bulky C-shaped POM frameworks, partial structural changes in the Ag···Ag distances and partial rotations and/or distortions of the $\{Ag_6\}$ octahedrons were allowed. Hence, we further investigated the structure of the $\{Ag_{27}\}$ nanocluster by analyzing the Fourier transformed EXAFS spectra of **Ag27** and **Ag27'** (see Supporting Information for details). A peak assignable to the Ag···Ag interactions of **Ag27'** was observed at 2.79±0.02 Å, which was slightly longer than that of **Ag27** (2.74±0.02 Å; Figure 3d). Notably, the coordination number (CN) in **Ag27** was considerably smaller (CN, 2.7±0.2; Table S1 and Figure S9) than the expected value according to the X-ray crystallographic analysis (suggested CN, 4.84; average *R*, 2.87 Å). Longer Ag···Ag distances were probably not observed in the EXAFS spectrum because of their broad distribution (Figure 3e). In contrast, the observed CN in **Ag27'** (CN, 4.9±0.2; Table S1 and Figure S10) was similar to the expected value based on the X-ray structure. These results indicate that several long Ag···Ag distances became shorter by the reaction with H_2, and as a result, the number of Ag atoms that of Ag···Ag distances around 2.79 Å likely increased. In **Ag27**, the Ag···Ag distances on the edge of the $\{Ag_6\}$ octahedron and the $\{Ag_9\}$ cores were in the range 2.7–3.0 Å (Figure 3e). In contrast, the Ag···Ag distances between the dioctahedral $\{Ag_9\}$ core and surrounding $\{Ag_6\}$ octahedrons (*e.g.*, Ag2···Ag24, Ag3···Ag22) were in the range 3.0–3.3 Å, indicating that the distances between these Ag atoms were shortened upon the reaction with H_2.

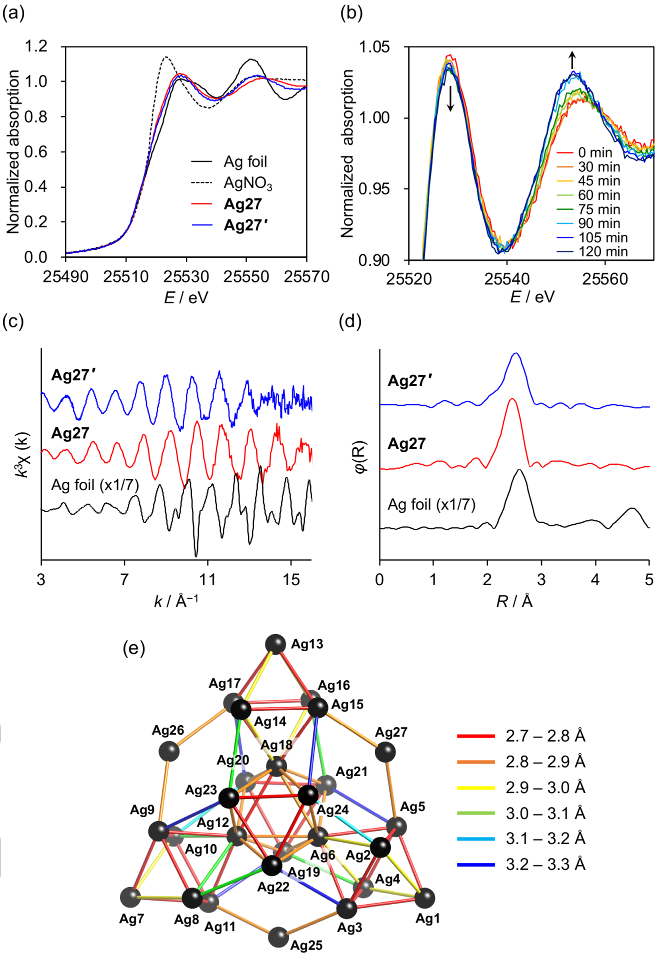

Figure 3. (a) Solid-state Ag K-edge XANES spectra of **Ag27**, **Ag27'**, Ag foil, and $AgNO_3$. (b) Monitoring of the reaction solution of **Ag27** and H_2 in DMF at 50°C by Ag K-edge XANES spectra. (c) Solid-state *k*-space and (d) Ag K-edge Fourier transformed EXAFS spectra of **Ag27**, **Ag27'**, and Ag foil (×1/7 scale). (e) Structure of the $\{Ag_{27}\}$ core in **Ag27**. The color codes of the sticks between Ag atoms indicate the range of the Ag···Ag distances.

These NMR, ESI mass, UV–vis, XAFS, and XPS studies revealed that two H_2 molecules were cleaved by **Ag27**, and the four protons and four electrons generated were stored on the POM frameworks and the internal $\{Ag_{27}\}$ nanocluster, respectively. Thus, the $\{Ag_{27}\}^{17+}$ nanocluster (**Ag27**) was reduced to $\{Ag_{27}\}^{13+}$ (**Ag27’**) by the reaction with H_2. Overall, the reaction of **Ag27** with H_2 can be expressed by the following equation (Eq. 1):

$$[\{Ag_{27}\}^{17+}(Si_6W_{54}O_{198})]^{31-} + 2H_2 \rightarrow [\{Ag_{27}\}^{13+}(H^+{}_4Si_6W_{54}O_{198})]^{31-} \quad \text{(Eq. 1)}$$

Typically, H_2 is heterolytically cleaved into H^+ and H^- at the interface between metal nanoparticles and metal oxide supports.[8] The H^- species on the metal nanoparticles supported on reducible metal oxides such as TiO_2 can be further dissociated into H^+ and two electrons, both of which migrate to the metal oxide surface (hydrogen spillover).[8,11] Since POMs are also reducible molecular metal oxides, POMs with polydisperse Pt(0) nanoparticles have been reported to cleave H_2 into two H^+ and two electrons, both of which are stored in the POM molecule to form a reduced POM (W^{5+}) species.[11d] The present **Ag27** system exhibited a unique reactivity; H_2 was cleaved into two H^+ and two electrons most likely through a heterolytic pathway at the interface between the $\{Ag_{27}\}$ nanocluster and the POMs, and the protons and electrons generated were stored on the POM surface and the mixed-valent $\{Ag_{27}\}^{17+}$ nanoclusters, respectively, in the hybrid. The density functional theory calculations showed that the natural charges of Ag atoms decreased while those of W atoms in POMs remained unchanged by the reaction of **Ag27** with two H_2 molecules (Figure S11), also supporting these experimental results. After removing the H_2 from the reaction solution, the UV–vis spectra of **Ag27’** did not change, and the electronic state of the $\{Ag_{27}\}$ nanocluster remained unaltered under Ar atmosphere (Figure S12). In contrast, when the solution was treated with O_2 at 50°C, the UV–vis spectra gradually changed and became similar to that of **Ag27**, although it did not return back to its original state completely.

In conclusion, we demonstrated that a molecular hybrid of an atomically precise Ag nanocluster and POMs can efficiently cleave H_2 into protons and electrons, which were stored on the POM frameworks and the mixed-valent $\{Ag_{27}\}^{17+}$ nanocluster, respectively. In particular, the POM ligands played important roles in this system by (i) significantly stabilizing the typically unstable Ag nanocluster to preserve its structure during the redox reaction with H_2, (ii) forming a unique interface between the Ag nanocluster and metal oxides for an efficient H_2 cleavage, and (iii) storing the generated protons on the negatively charged basic surface. We believe that these are important results that will open new avenues to explore the unique reactivity and catalytic activity of hybrid materials of metal nanoclusters and POMs.[23]

Acknowledgements

We gratefully acknowledge the financial support from JST PRESTO Grant Number JPMJPR18T7 and JPMJPR19T9, JSPS KAKENHI Grant Numbers 20H02749, 20H04659, 17H03037, and the JSPS Core-to-Core program. A part of the computations was performed using Research Center for Computational Science, Okazaki, Japan. The XAFS measurements were conducted at SPring-8 with the approval of the Japan synchrotron Radiation Research Institute (Proposal number: 2020A1410). We thank Dr. T. Yabe (Univ. of Tokyo) and Dr. J. Hirayama (TMU) for help with XAFS measurements.

Conflict of interest

The authors declare no conflict of interest.

Keywords: cluster compounds • hydrogen • polyoxometalates • silver nanoclusters

[1] a) R. Jin, C. Zeng, M. Zhou, Y. Chen, *Chem. Rev.* **2016**, *116*, 10346–10413; b) I. Chakraborty, T. Pradeep, *Chem. Rev.* **2017**, *117*, 8208–8271; c) Y. Du, H. Sheng, D. Astruc, M. Zhu, *Chem. Rev.* **2020**, *120*, 526–622; d) Y.-P. Xie, Y.-L. Shen, G.-X. Duan, J. Han, L.-P. Zhang, X. Lu, *Mater. Chem. Front.* **2020**, *4*, 2205–2222; e) G.-G. Luo, Q.-L. Guo, Z. Wang, C.-F. Sun, J.-Q. Lin, D. Sun, *Dalton Trans.* **2020**, *49*, 5406–5415; f) Y. Liu, X. Chai, X. Cai, M. Chen, R. Jin, W. Ding, Y. Zyu, *Angew. Chem. Int. Ed.* **2018**, *57*, 9775–9779; *Angew. Chem.* **2018**, *130*, 9923–9927.

[2] a) D. Sun, G.-G. Luo, N. Zhang, R.-B. Huang, L.-S. Zheng, *Chem. Commun.* **2011**, *47*, 1461–1463; b) C. P. Joshi, M. S. Bootharaju, M. J. Alhilaly, O. M, Bakr, *J. Am. Chem. Soc.* **2015**, *137*, 11578–11581; c) R. S. Dhyal, J.-H. Liao, Y.-C. Liu, M.-H. Chiang, S. Kahlal, J.-Y. Saillard, C. W. Liu, *Angew. Chem. Int. Ed.* **2015**, *54*, 3702–3706; *Angew. Chem.* **2015**, *127*, 3773–3777; d) L. Ren, P. Yuan, H. Su, S. Malola, S. Lin, Z. Tang, B. K. Teo, H. Häkkinen, *J. Am. Chem. Soc.* **2017**, *139*, 13288–13291; e) A. Desireddy, B. E. Conn, J. Guo, B. Yoon, R. N. Barnett, B. M. Monahan, K. Kirschbaum, W. P. Griffith, R. L. Whetten, U. Landman, T. P. Bigioni, *Nature* **2013**, *501*, 399–402; f) H. Yang, Y. Wang, H. Huang, L. Gell, L. Lehtovaara, S. Malola, H. Häkkinen, N. Zheng, *Nat. Commun.* **2013**, *4*, 2422; g) W. Du, S. Jin, L. Xiong, M. Chen, J. Zhang, X. Zou, Y. Pei, S. Wang, M. Zhu, *J. Am. Chem. Soc.* **2017**, *139*, 1618–1624; h) H. Yang, J. Yan, Y. Wang, H. Su, L. Gell, X. Zhao, C. Xu, B. K. Teo, H. Häkkinen, N. Zheng, *J. Am. Chem. Soc.* **2017**, *139*, 31–34; i) S.-F. Yuan, Z.-J. Guan, W.-D. Liu, Q.-M. Wang, *Nat. Commun.* **2019**, *10*, 4032; j) K.-G. Liu, X.-M. Gao, T. Liu, M.-L. Hu, D.-E. Jiang, *J. Am. Chem. Soc.* **2020**, *142*, 16905–16909.

[3] a) M. T. Pope, *Heteropoly and Isopoly Oxometalates*, Springer, Berlin, 1983; b) M. Sadakane, E. Steckhan, *Chem. Rev.* **1998**, *98*, 219– 238; c) H. Lv, Y. V. Geletii, C. Zhao, J. W. Vickers, G. Zhu, Z. Luo, J. Song, T. Lian, D. G. Musaev, C. L. Hill, *Chem. Soc. Rev.* **2012**, *41*, 7572–7589; d) S.-S. Wang, G.-Y. Yang, *Chem. Rev.* **2015**, *115*, 4893–4962; e) I. A. Weinstock, R. E. Schreiber, R. Neumann, *Chem. Rev.* **2018**, *118*, 2680–2717; f) H. N. Miras, J. Yan, D.-L. Long, L. Cronin, *Chem. Soc. Rev.* **2012**, *41*, 7403–7430; g) M. Lechner, R. Gütte, C. Streb, *Dalton Trans.* **2016**, *45*, 16716–16726; h) K. Suzuki, N. Mizuno, K. Yamaguchi, *ACS Catal.* **2018**, *8*, 10809–10825; i) S. Uchida, *Chem. Sci.* **2019**, *10*, 7670–7679.

[4] a) K. Suzuki, Y. Kikukawa, S. Uchida, H. Tokoro, K. Imoto, S. Ohkoshi, N. Mizuno, *Angew. Chem. Int. Ed.* **2012**, *51*, 1597–1601; *Angew. Chem.* **2012**, *124*, 1629–1633; b) K. Suzuki, F. Tang, Y. Kikukawa, K. Yamaguchi, N. Mizuno, *Angew. Chem. Int. Ed.* **2014**, *53*, 5356–5360; *Angew. Chem.* **2014**, *126*, 5460–5464; c) T. Minato, K. Suzuki, K. Yamaguchi, N. Mizuno, *Angew. Chem. Int. Ed.* **2016**, *55*, 9630–9633; *Angew. Chem.* **2016**, *128*, 9782–9785; d) T. Minato, K. Suzuki, Y. Ohata, K. Yamaguchi, N. Mizuno, *Chem. Commun.* **2017**, *53*, 7533–7536; e) K. Suzuki, T. Minato, N. Tominaga, I. Okumo, K. Yonesato, N. Mizuno, K. Yamaguchi, *Dalton. Trans.* **2019**, *48*, 7281–7289; f) S. Sasaki, K. Yonesato, N. Mizuno, K. Yamaguchi, K. Suzuki, *Inorg. Chem.* **2019**, *58*, 7722–7729; g) C. Li, A. jimbo, K. Yamaguchi, K. Suzuki, *Chem. Sci.* **2021**, *12*, 1240–1244.

[5] K. Yonesato, H. Ito, H. Itakura, D. Yokogawa, T. Kikuchi, N. Mizuno, K. Yamaguchi, K. Suzuki, *J. Am. Chem. Soc.* **2019**, *141*, 19550–19554.

[6] K. Yonesato, H. Ito, D. Yokogawa, K. Yamaguchi, K. Suzuki, *Angew. Chem. Int. Ed.* **2020**, *59*, 16361–16365; *Angew. Chem.* **2020**, *132*, 16503–16507.

[7] a) X.-Y. Dong, Z.-W. Gao, K.-F. Yang, W.-Q. Zhang, L.-W. Xu, *Catal. Sci. Technol.* **2015**, *5*, 2554–2574; b) J. T. Gleaves, A. G. Sault, R. J. Madix, J. Ebners, *J. Catal.* **1990**, *121*, 202–218; c) R. B. Grant, R. M. Lambert, *J. Catal.* **1985**, *92*, 364–375; d) T. Mitsudome, S. Arita, H. Mori, T. Mizugaki, K. Jitsukawa, K. Kaneda, *Angew. Chem. Int. Ed.* **2008**, *47*, 7938–7940; *Angew. Chem.* **2008**, *120*, 8056–8058; e) Y. Mikami, A. Noujima, T. Mitsudome, T. Mizugaki, K. Jitsukawa, K. Kaneda, *Chem. Lett.* **2010**, *39*, 223–225; f) T. Mitsudome, Y. Mikami, H. Mori, S. Arita, T. Mizugaki, K. Jitsukawa, K. Kaneda, *Chem. Commun.* **2009**, 3258–3260; g) K. Shimizu, K. Ohshima, A. Satsuma, *Chem. Eur. J.* **2009**, *15*, 9977–9980; h) T. Mitsudome, Y. Mikami, M. Matoba, T. Mizugaki, K. Jitsukawa, K. Kaneda, *Angew. Chem. Int. Ed.* **2012**, *51*, 136–139; *Angew. Chem.* **2012**, 124, 140–143.

[8] a) L. Zhang, M. Zhou, A. Wang, T. Zhang, *Chem. Rev.* **2020**, *120*, 683–733; b) R. Prins, *Chem. Rev.* **2012**, *112*, 2714–2738; c) J. Zhang, L. Li, X. Huang, G. Li, *J. Mater. Chem.* **2012**, *22*, 10480–10487.

[9] a) K. Nagata, T. Murosaki, T. Agou, T. Sasamori, T. Matsuo, N. Tokitoh, *Angew. Chem. Int. Ed.* **2016**, *55*, 12877–12880; *Angew. Chem.* **2016**, *128*, 13069–13072; b) E. von Grotthuss, M. Diefenbach, M. Bolte, H. W. Lerner, M. C. Holthausen, M. Wagner, *Angew. Chem. Int. Ed.* **2016**, *55*, 14067–14071; *Angew. Chem.* **2016**, *128*, 14273–14277.

[10] a) G. C. Welch, R. R. S. Juan, J. D. Masuda, D. W. Setephan, *Science* **2006**, *314*, 1124–1126; b) G. C. Welch, D. W. Stephan, *J. Am. Chem. Soc.* **2007**, *129*, 1880–1881.

[11] a) P. Sabatier, *Ind. Eng. Chem.* **1926**, *18*, 1005; b) P. Serna, A. Corma, *ACS Catal.* **2015**, *5*, 7114–7121; c) A. M. Smith, R. Whyman, *Chem. Rev.* **2014**, *114*, 5477; d) S. Itagaki, K. Yamaguchi, N. Mizuno, *Chem. Mater.* **2011**, *23*, 4102–4104.

[12] a) M. Ito, T. Ikariya, *Chem. Commun.* **2007**, 5134–5142; b) Y. Misumi, H. Seino, Y. Mizobe, *J. Am. Chem. Soc.* **2009**, *131*, 14636–14637.

[13] P. Spies, S. Schwendemann, S. Lange, G. Kehr, R. Fröhlich, G. Erker, *Angew. Chem. Int. Ed.* **2008**, *47*, 7543–7546; *Angew. Chem.* **2008**, *120*, 7654–7657.

[14] a) S. Shima, O. Pilak, S. Vogt, M. Schick, M. S. Stagni, W. M. Klaucke, E. Warkentin, R. K. Thauer, U. Ermler, *Science* **2008**, *321*, 572–575; b) W. Lubitz, H. Ogata, O. Rüdiger, E. Reijerse, *Chem. Rev.* **2014**, *114*, 4081; c) H. Land, M. Senger, G. Berggren, S. T. Stripp, *ACS Catal.* **2020**, *10*, 7069–7086.

[15] a) S. Ogo, K. Ichiklawa, T. Kishima, T. Matsumoto, H. Nakai, K. Kusaka, T. Ohhara, *Science* **2013**, *339*, 682–684; b) T. Liu, X. Wang, C. Hoffmann, D. L. DuBois, Morris Bullock, *Angew. Chem. Int. Ed.* **2014**, *53*, 5300–5304; *Angew. Chem.* **2014**, *126*, 5404–5408.

[16] a) Y. Zhu, H. Qian, B. A. Drake, R. Jin. *Angew. Chem. Int. Ed.* **2010**, *49*, 1295–1298; *Angew. Chem.* **2010**, *122*, 1317–1320; b) G. Li, D.-E. Jiang, S. Kumar, Y. Chen, R. Jin, *ACS Catal* **2014**, *4*, 2463–2469.

[17] S. Takano, H. Hirai, S. Muramatsu, T. Tsukuda, *J. Am. Chem. Soc.* **2018**, *140*, 8380–8383.

[18] a) M. S. Bootharaju, R. Dey, L. E. Gevers, M. N. Hedhili, J.-M. Basset, O. M. Bakr, *J. Am. Chem. Soc.* **2016**, *138*, 13770–13773; b) M. Jash, E. Khatun, P. Chakraborty, C. Sudhakar, T. Pradeep, *J. Phys. Chem. C* **2020**, *124*, 20569 –20577.

[19] E. Papaconstantinou, *Chem. Soc. Rev.* **1989**, *18*, 1–31.

[20] HOMO and HOMO−1 of **Ag27** were superatomic orbitals that possessed p-like symmetry and dz^2-like symmetry, respectively. The disk-like distorted shape of {Ag$_{27}$} nanocluster likely caused the lower dz^2-like orbital energy and higher p-like orbital energy, which resulted in the unique superatomic configuration with 10 valence electrons.

[21] a) S. Yamazoe, T. Tsukuda, *Bull. Chem. Soc. Jpn.* **2019**, *92*, 193–204; b) T. Omoda, S. Takano, S. Yamazoe, K. Koyasu, Y. Negishi, T. Tsukuda, *J. Phys. Chem. C* **2018**, *122*, 13199–13204.

[22] The E_0 values for Ag foil and AgNO$_3$ were 25516.0 and 25518.5 eV, respectively.

[23] In the presence of a catalytic amount of **Ag27** (0.7 mol%) under H$_2$ (1 atm), 4-nitrobenzonitrile was efficiently reduced by irradiation of visible light (λ > 400 nm), selectively affording the corresponding azobenzene (Figure S13). In this case, byproducts such as the corresponding azoxybenzene and aniline were hardly detected. Since the reaction hardly proceeded in the absence of photo-irradiation or **Ag27**, it is clear that **Ag27** functions as a visible-light-responsive photocatalyst. Although the reaction proceeded to some extent in the absence of H$_2$, the fact that the reaction proceeded more efficiently in the presence of H$_2$ is noteworthy. Hence, the nitroarene reduction is considered to be proceeded with H$_2$ as the electron and proton sources. Based on the DFT studies and the above-mentioned experimental results, we consider that the key step for this reaction is the visible-light-induced electron transfer from {Ag$_{27}$} nanocluster to the POM frameworks. The electrons stored in {Ag$_{27}$} by the cleavage of H$_2$ (or from other electron sources) were possibly transferred to the POM framework by photo-irradiation, which successfully reduced the nitroarene to form the corresponding azobenzene.

Entry for the Table of Contents

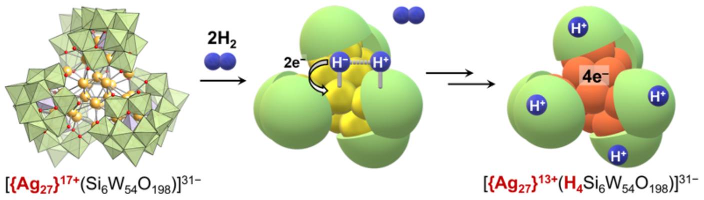

A molecular hybrid of an atomically precise mixed-valent $\{Ag_{27}\}^{17+}$ nanocluster and polyoxometalate (POM) ligands exhibited unique reactivity, efficiently cleaving dihydrogen (H_2) into protons and electrons, and the protons and electrons generated are stored on the POM surface and the mixed-valent $\{Ag_{27}\}^{17+}$ nanoclusters, respectively.

Institute and/or researcher Twitter usernames: ((optional))